Leaf Recognition Based on the Combination of Wavelet Transform and Gaussian Interpolation[1]

Xiao Gu[1], Ji-Xiang Du[1,2], and Xiao-Feng Wang[1]

[1] Institute of Intelligent Machines, Chinese Academy of Sciences, P.O.Box 1130, Hefei, Anhui 230031, China
[2] Department of Automation, University of Science and Technology of China, Hefei 230027, China
{xgu, du_jx, xfwang}@iim.ac.cn

Abstract: In this paper, a new approach for leaf recognition using the result of segmentation of leaf's skeleton based on the combination of wavelet transform (WT) and Gaussian interpolation is proposed. And then the classifiers, a nearest neighbor classifier (1-NN), a k -nearest neighbor classifier (k-NN) and a radial basis probabilistic neural network (RBPNN) are used, based on run-length features (RF) extracted from the skeleton to recognize the leaves. Finally, the effectiveness and efficiency of the proposed method is demonstrated by several experiments. The results show that the skeleton can be successfully and obviously extracted from the whole leaf, and the recognition rates of leaves based on their skeleton can be greatly improved.

1 Introduction

Plant recognition by computers automatically is a very important task for agriculture, forestry, pharmacological science, and etc. In addition, with the deterioration of environments, more and more rare plant species are at the margin of extinction. Many of rare plants have died out. So the investigation of the plant recognition can contribute to environmental protection. At present, plant recognition usually adopts following classification methods, such as color histogram, Fourier transform (FT), morphologic anatomy, cell biology, etc. [1].

Plant recognition can be performed in terms of the plants' shape, flowers, and leaves, barks, seeds, and so on. Nevertheless, most of them cannot be analyzed easily because of their complex 3D structures if based on simple 2D images. Therefore, in this paper, we study plant recognition by its leaf, exactly by leaf's skeleton. So we can use leaves skeleton as their texture features to recognize them.

In this paper, a new method of segmenting leaf's skeleton is proposed. That is, the combination of wavelet transform and Gaussian interpolation is used to extract the leaf's contour and venation as well as skeleton. Usually, the wavelet transform is of the capability of mapping an image into a low-resolution image space and a series of detail image spaces. However, ones only keep an eye on the low-resolution images,

[1] This work was supported by the National Natural Science Foundation of China (Nos.60472111 and 60405002).

D.S. Huang, X.-P. Zhang, G.-B. Huang (Eds.): ICIC 2005, Part I, LNCS 3644, pp. 253 – 262, 2005.

while the detail images are ignored. For the majority of images, their detail images indicate the noise or uselessness of the original ones. But the so-called noise of leaf's image is just the leaf's skeleton. So, we intentionally adopt the detail images to produce leaf's skeleton. And then, the extraction of texture features will be carried out based on the leaf's skeleton. After that, we derive run-length features (RF) from leaf's skeleton, which can reflect the directivity of texture in the image. Therefore, after computing these features of leaves, different species of plants can be classified by using three classifiers such as 1-NN, *k*-NN and radial basis probabilistic neural network (RBPNN) [2].

The rest of this paper is organized as follows: Section 2 reviews the WT, and Section 3 introduces how to use the combination of WT and Gaussian interpolation to segment the skeleton of leaf, and gives the corresponding algorithm. Section 4 reports some experimental results on leaf recognition. Finally, some concluding remarks are included in Section 5.

2 The Review of Wavelet Transform

The wavelet transform (WT), a linear integral transform that maps $L^2(\mathbb{R}) \to L^2(\mathbb{R}^2)$, has emerged over the last two decades as a powerful new theoretical framework for the analysis and decomposition of signals and images at multi-resolutions [3]. Moreover, due to its both locations in time/space and in frequency, this transform is to completely differ from Fourier transform [4,5].

2.1 Wavelet Transform in 1D

The wavelet transform is defined as decomposition of a signal $f(t)$ using a series of elemental functions called as wavelets and scaling factors, which are created by scaling and translating a kernel function $\psi(t)$ referred to as the mother wavelet:

$$\psi_{ab}(t) = \frac{1}{\sqrt{a}}\psi(\frac{t-b}{a}) \qquad where \quad a,b \in \mathbb{R}, a \neq 0 \ . \tag{1}$$

Thus, the continuous wavelet transform (CWT) is defined as the inner product:

$$W_f(a,b) = \int_{-\infty}^{\infty} \psi_{ab}(t)\bar{f}(t)dt = \langle \psi_{ab}, f \rangle \ . \tag{2}$$

And, the discrete wavelet representation (DWT) can be defined as:

$$W_f^d(j,k) = \int_{-\infty}^{\infty} \psi_{j,k}(x)\bar{f}(x)dt = \langle \psi_{j,k}, f \rangle \qquad j,k \in \mathbb{Z} \ . \tag{3}$$

Thus, the DWT of $f(x)$ can be written as:

$$W_{\varphi}(j_0,k)=\sum_x f(x)\varphi_{j_0,k}(x)\ . \tag{4}$$

$$W_{\psi}(j,k)=\sum_x f(x)\psi_{j,k}(x)\ . \tag{5}$$

where the wavelet and scaling functions are:

$$\psi_{j,k}(x)=2^{-\frac{j}{2}}\psi(2^{-j}x-k)\ . \tag{6}$$

$$\varphi_{j,k}(x)=2^{-\frac{j}{2}}\varphi(2^{-j}x-k)\ . \tag{7}$$

where j is the scale factor, and k is the shifting factor.

Therefore, 1D wavelet transform of a discrete signal is equal to passing the signal through a pair of low-pass and high-pass filters, followed by a down-sampling operator with factor 2 [6].

2.2 Wavelet Transform in 2D

Simply by applying two 1D transforms separately, 2D wavelet transform of an image $I = A_0 = f(x, y)$ of size $M \times N$ is then:

$$A_j=\sum_x\sum_y f(x,y)\varphi(x,y)\ . \tag{8}$$

$$D_{j1}=\sum_x\sum_y f(x,y)\psi^H(x,y)\ . \tag{9}$$

$$D_{j2}=\sum_x\sum_y f(x,y)\psi^V(x,y)\ . \tag{10}$$

$$D_{j1}=\sum_x\sum_y f(x,y)\psi^D(x,y)\ . \tag{11}$$

That is, four quarter-size output sub-images, A_j, D_{j1}, D_{j2}, and D_{j3}, are generated by convolving its rows and columns with h_l and h_h, and down-sampling its columns or rows, as shown in Figure 1.

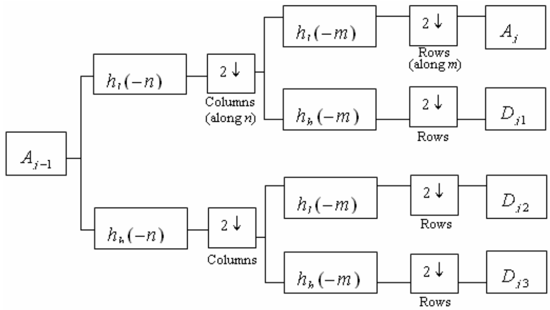

Fig. 1. Block diagram of 2-D discrete wavelet transform

Here, h_l and h_h are the low-pass and high-pass filters, respectively, j is the decomposition or reconstruction scale, $\downarrow 2{,}1(\uparrow 2{,}1)$ represents sub-sampling along the rows (columns) [7]. A_j, an approximation component containing its low-frequency information, is obtained by low-pass filtering, and it is therefore referred to as the low-resolution image at scale j. The detail images D_{ji} are obtained by high-pass filtering in specific direction that contains directional detail information in high-frequency at scale j [8]. The set of sub-images at several scales, $\{A_d, D_{ji}\}_{i=1,2,3,j=1...d}$, are known as the approximation and the detail images of the original image I, respectively [7].

3 Application of the Combination of Wavelet Transform and Gaussian Interpolation

In our study, WT is used to decompose leaf's images and produce low-resolution images and a series of detail images. Usually, the detail information distributed in three directions is the horizontal, vertical and diagonal details in corresponding three images. Generally, because of usefulness of the approximation of the image, these detail images are removed at the effort of blurring the image, removing noise, and detecting edges from image, etc.

However, the details where there exists leaf's contour and venation are the key of the whole image processing. Leaf's skeleton will be produced from these detail images by a synthesized manner. Here, a series of detail images will be obtained based on wavelet transformation. If a single image is decomposed for several times, then the number of detail images will be trebled. Thus, the total number of statistical features gotten from these detail images will be increased promptly. In addition, there also exists the redundant information in these features. Therefore, we will add Gaussian interpolation to the three detail images, D_{j1} D_{j2} and D_{j3} , and then reconstruct them at each scale after decomposition. At the same time, this operation will bring us the vivid leaf's skeleton at different scales. Thus, all the details distributed over three images will be focused on only a single image. It will shrink the

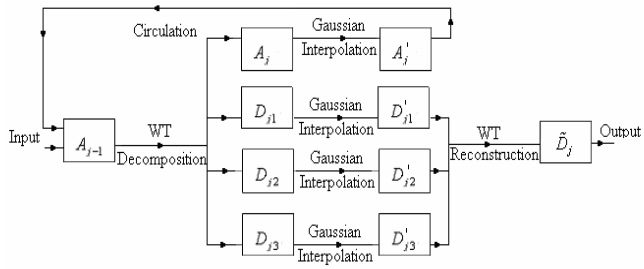

Fig. 2. Block diagram of application of WT to segmentation of leaf's skeleton

range for feature extraction subsequently. Consequently, the reconstructed detail images and the leaf's skeletons can be defined as $\tilde{D}_j$. All of these are clearly shown in Figure 2.

After getting the images $\{\tilde{D}_j\}$ of leaf's skeleton, we can extract texture features from them to recognize the leaves. Here we use the run-length features $(l, \ b, \ \theta)$, which is the sequence of l pixels with gray scale b at direction θ and $N(l, \ b, \ \theta)$ is generally defined to describe the number of run $(l, \ b, \ \theta)$ in the image. Let L denote the gray scale of image, and N_l denote the number of l. And the denominator in the following formulae will normalize these features.

The measure of short runs

$$SR = \frac{\sum_{b=1}^{L}\sum_{l=1}^{N_l}\frac{1}{l^2}N(l, \ b, \ \theta)}{\sum_{b=1}^{L}\sum_{l=1}^{N_l}N(l, \ b, \ \theta)} . \tag{12}$$

The measure of long runs

$$LR = \frac{\sum_{b=1}^{L}\sum_{l=1}^{N_l}l^2 N(l, \ b, \ \theta)}{\sum_{b=1}^{L}\sum_{l=1}^{N_l}N(l, \ b, \ \theta)} . \tag{13}$$

Distribution of gray scales

$$DG = \frac{\sum_{b=1}^{L}[\sum_{l=1}^{N_l}N(l, \ b, \ \theta)]^2}{\sum_{b=1}^{L}\sum_{l=1}^{N_l}(l, \ b, \ \theta)} . \tag{14}$$

Distribution of lengths

$$DL = \frac{\sum_{l=1}^{N_l}[\sum_{b=1}^{L} N(l, \quad b, \quad \theta)]^2}{\sum_{b=1}^{L}\sum_{l=1}^{N_l}(l, \quad b, \quad \theta)} . \tag{15}$$

Percentage of runs

$$PR = \frac{\sum_{b=1}^{L}\sum_{l=1}^{N_l} N(l, \quad b, \quad \theta)}{N_1 \times N_2} . \tag{16}$$

Now, we can separate the algorithm into two main parts. Part 1 is the segmentation of leaf's skeleton by WT, and Part 2 is the extraction of features. The detailed steps of this algorithm can be stated as follows:

Part 1: Skeleton segmentation stage

Step 1. Input the original leaf's image I .

Step 2. If I is a color image, we can turn it into a gray scale image and denote it as $A_0 = A_0^{'}$. Or just let $A_0 = A_0^{'} = I$, and then turn to Step 3.

Step 3. Set the parameters of WT, like the levels of WT, the wavelet's name and its corresponding coefficients. Denote the variable for circulation as j , and let $j = 1$.

Step 4. Decompose $A_{j-1}^{'}$ to get four images (A_j , D_{j1} , D_{j2} and D_{j3}) by WT.

Step 5. Adding Gaussian interpolation to A_j , D_{j1} , D_{j2} and D_{j3} , to produce $A_j^{'}$, $D_{j1}^{'}$, $D_{j2}^{'}$ and $D_{j3}^{'}$.

Step 6. Reconstruct $D_{j1}^{'}$, $D_{j2}^{'}$ and $D_{j3}^{'}$ to get the image of leaf's skeleton $\tilde{D}_j$.

Part 2: Feature extraction stage

Step 7. Extracting the run-length features (SR , LR , DG , DL and PR) from the image $\tilde{D}_j$. Meanwhile, save these features to a data file.

Step 8. If j equals to the parameter of levels of WT, turn to Step 8. Otherwise let $j = j + 1$, and then turn to Step 4.

Step 9. End, and output the data file which saves the features.

4 Experiments and Results

All the following experiments are programmed by Microsoft Visual C++ 6.0, and run on Pentium 4 with the clock of 2.6 GHz and the RAM of 256M under Microsoft windows XP environment. Meanwhile, all of the results for the following Figures and Tables are obtained by the experiments more than 50 times, and then are averaged.

This database of the leaf images is built by us in our lab by the scanner and digital camera, including twenty species (as shown in Figure 3).

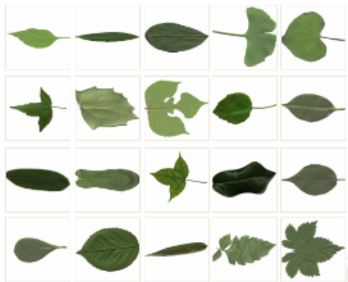

Fig. 3. Twenty species of leaf images

Before processing, the colored images will be turned into gray-scale images (as shown in Figure 4), ignoring the color information, since the majorities of leaves are green. In practice, the variety of the change of nutrition, water, atmosphere and season can cause the change of the color.

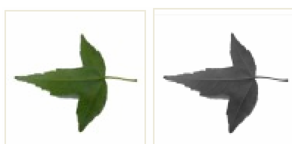

Fig. 4. The pre-processed images: Original image and Gray-scale image

After pre-processing procedure, the gray-scale images will be decomposed by WT of depth 3 using a biorthogonal spline wavelet of order 2 [9]. The decomposed images at each scale j, including approximate images A_j, horizontal detail images D_{j1}, vertical detail images D_{j2}, and diagonal detail images D_{j3}, $j = 1,2,3$, are shown in Figure 5. After every wavelet is decomposed, by adding Gaussian interpolation, the results as images $\{A_j^{'}, D_{j1,}^{'} D_{j2,}^{'} D_{j3,}^{'}\}_{j=1,2,3}$ can be seen in Figure 6. And Figure 7 clearly shows the reconstructed images $\{\tilde{D}_j\}_{j=1,2,3}$, from which we can see the leaf's skeleton obviously.

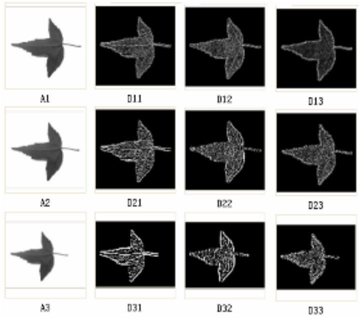

Fig. 5. Images that are decomposed by wavelet transform

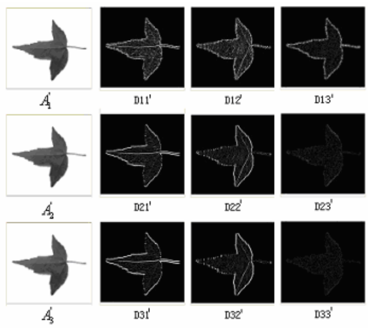

Fig. 6. Adding Gaussian interpolation to wavelet decomposition

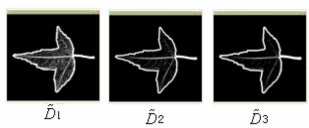

Fig. 7. The leaf's skeleton derived by reconstructing detail images after Gaussian interpolation at different scale j

After the segmentation of leaf's skeleton, three reconstructed detail images $\{\tilde{D}_j\}_{j=1,2,3}$ of a single image are generated. There are 60 ($5\times4\times3$) features of run-length for extraction. And assume that 1-NN, k-NN and RBPNN [10,11] with the recursive least square back propagation algorithm (RLSBPA) [12,13-17], are respectively used for recognition and comparison. The results are respectively shown in Figure 8 and Table 1.

It is shown in Figure 8 that, the correct rate of using original image for leaf recognition can only reach 60 percent or somewhat more than 75 percent, and the instance of only using WT can get an increase of 10 percent. Finally, using the method proposed in this paper, i.e., a combination of WT and Gaussian interpolation, the result is the best, which can be close to 95 percent. Moreover, we can carefully

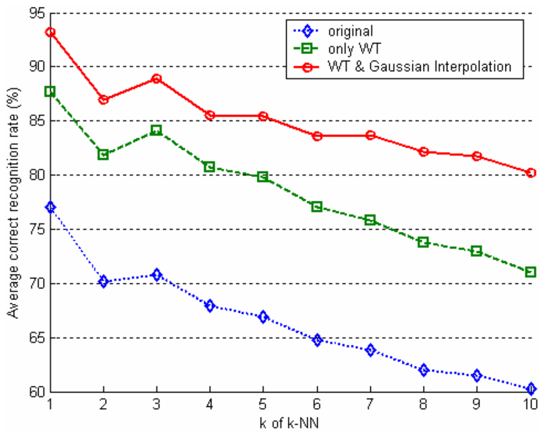

Fig. 8. *k vs.* the average correct recognition rates of using three different classification methods

Table 1. The performance comparison of different classifiers

Classifiers	1-NN	k-NN (k=5)	RBPNN
Average correct recognition rate (%)	93.1702	85.4681	91.1809

find that, with the increase of k, the downtrend of the correct recognition rate of using WT and Gaussian interpolation is slower than the former. It tells us that the stability of this method is the best. And Table 1 gives the distribution of the average correct rate by using our method.

5 Conclusions

This paper proposed a new wavelet decomposition and Gaussian interpolation method, which not only successfully separates the contour but also separates the venation, i.e., the skeleton of the whole leaf. Then, run-length features (RF) were used to perform the recognition of leaves by different classifiers such as 1-NN, k-NN and RBPNN. The experimental results found that our method can obviously segment the leaf's skeleton, and the correct recognition rate of using features extracted from the skeleton is more improved than other methods.

References

1. Du, J.X., Wang, X.F., Huang, D.S.: Automatic Plant Leaves Recognition System Based on Image Processing Techniques. Technical Report. Institute of Intelligent Machines. Chinese Academy of Sciences. (2004)
2. Huang, D.S, Ma, S.D.: Linear and Nonlinear Feed-Forward Neural Network Classifiers: A Comprehensive Understanding. Journal of Intelligent System 9(1) (1999) 1 - 38

3. Vetterli, M., Kovacevic, J.: Wavelets and Subband Coding. Prentice Hall. Englewood Cliffs. New Jersey. (1995)
4. Akansu, Ali N., Richard, A. Haddad: Multiresolution Signal Decomposition: Transforms, Subbands, Wavelets. Academic Press. Inc. (1992)
5. Vetterli, M., Herley, C.: Wavelets and Filter Banks: Theory and Design. IEEE Trans. on Signal Proc. Vol. 40. (1992) 2207-2231
6. Ahmadian, A. Mostafa: An Efficient Texture Classification Algorithm Using Gabor Wavelet. Proceedings of the 25th Annual International Conference of the IEEE EMBS. Cancum. Mexico. (2003)
7. Busch, A., Boles, W., Sridharan, S.: Logarithmic Quantisation of Wavelet Coefficients for Improved Texture Classification Performance. The International Conference on Acoustics, Speech, and Signal Processing. Proceedings. (ICASSP 2004)
8. Wouwer, G. Van de, Scheunders, P., Dyck, D. Van: Statistical Texture Characterization from Discrete Wavelet Representations. IEEE Transactions on Image Processing. (1999)
9. Unser, M., Aldroubi, A., Eden, M.: A Family of Polynomial Spline Wavelet Transforms. Signal Processing. Vol. 30. (1993) 141 - 162
10. Huang, D.S.: Radial Basis Probabilistic Neural Network: Model and Application. International Journal of Pattern Recognition and Artificial Intelligence. 13(7) (1999) 1083 - 1101
11. Zhao, W.B., Huang, D.S.: The Structure Optimization of Radial Basis Probabilistic Networks Based on Genetic Agorithm. The 2002 IEEE World Congress on Computational Intelligence. IJCNN02. (2002) 1086 - 1091
12. Huang, D.S.: Systematic Theory of Neural Networks for Pattern Recognition (in Chinese). Publishing House of Electronic Industry of China. Beijing. (1996) 49 - 51
13. Huang, D.S., Zhao, W.B.: Determining the Centers of Radial Basis Probabilities Neural Networks by Recursive Orthogonal Least Square Algorithms. Applied Mathematics and Computation. Vol. 162. No.1. (2005) 461 - 473
14. Huang, D.S., Ma, S.D.: A New Radial Basis Probabilistic Neural Network Model. The 3rd Int. Conf on Signal Processing (ICSP) Proceedings. Beijing. China. (Oct. 14-18 1996) 1449 - 1452
15. Huang, D.S.: The Local Minima Free Condition of Feedforward Neural Networks for Outer-Supervised Learning. IEEE Trans on Systems, Man and Cybernetics. Vol.28B. No.3. (1998) 477 - 480
16. Huang, D.S.: Application of Generalized Radial Basis Function Networks to Recognition of Radar Targets. International Journal of Pattern Recognition and Artificial Intelligence. Vol.13. No.6. (1999) 945 - 962
17. Huang, D.S.: The Bottleneck Behaviour in Linear Feedforward Neural Network Classifiers and Their Breakthrough. Journal of Computer Science and Technology. Vol.14. No.1. (1999) 34 - 43